LANGMUIR

Article

pubs.acs.org/Langmuir

Digestive Ripening of Au Nanoparticles Using Multidentate Ligands

Puspanjali Sahu,[†] Jayesh Shimpi,[†] Han Ju Lee,[‡] T. Randall Lee,[‡] and Bhagavatula L. V. Prasad*[,†]

[†]Materials Chemistry Division, National Chemical Laboratory, Dr. Homi Bhabha Road, Pune 411008, India

[‡]Department of Chemistry, University of Houston, Houston, Texas 77204-5003, United States

Supporting Information

ABSTRACT: The efficiency of multidentate ligands as digestive ripening (DR) agents for the preparation of monodisperse Au nanoparticles (NPs) was investigated. This systematic investigation was performed using ligands possessing one, two, or three thiol moieties as ligands/DR agents. Our results clearly establish that among the different ligands, monodentate ligands and the use of temperature in the range of 60−120 °C offer the best conditions for DR. In addition, when DR was carried out at lower temperatures (e.g., 60 °C), the NP size increased as the number of thiol groups per ligand increased. However, in the case of ligands possessing two and three thiol moieties, when they were heated with polydispersed particles at higher temperatures (120 or 180 °C), the etching process dominated, which affected the quality of the NPs in terms of their monodispersity. We conclude that the temperature-dependent strength of the interaction between the ligand headgroup and the NP surface plays a vital role in controlling the final particle sizes.

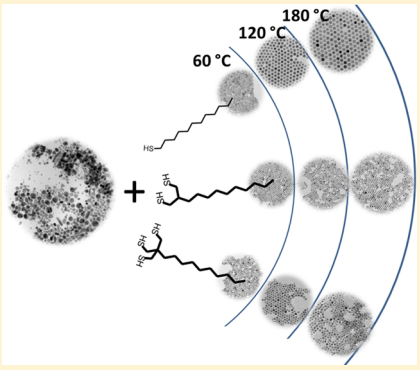

INTRODUCTION

In the realm of bottom−up approaches to nanoparticle (NP) synthesis, the preparation of monolayer-protected particles using two-phase reduction methods with organic molecules/ligands as capping or passivating agents has made a huge impact.[1−3] The convenience with which these monolayer-protected particles can be purified/handled, and more importantly, the possibility of modifying the surface with many different ligands has made this procedure one of the most widely used. The range of monolayer-protected NP syntheses has been further extended/strengthened with procedures such as size focusing, digestive ripening (DR), or inverse Ostwald ripening, which lead to the formation of nearly monodispersed particles.[4−6] Quite interestingly, with these methods, the size distribution of a polydispersed NP system becomes narrower with a concomitant reduction in the average particle size. The fact that these procedures offer tremendous control over the size and size distributions of NPs, without requiring any further size-selective separation, renders them attractive and useful. Furthermore, these procedures seem to involve a step/process in which the smaller particles grow in size and the larger particles dissolve, which is in contrast to traditional mechanisms such as Ostwald ripening. Thus, there is tremendous interest in understanding the mechanism of size and size control via these methods because they cannot be explained completely with the conventional nucleation and growth mechanisms or surface energy arguments alone.[7]

Although reports on the preparation of NPs of different kinds via DR are ubiquitous in the literature, systematic studies carried out to understand the mechanism are comparatively few.[9,10] Furthermore, a convincing theory/model that rationalizes all of the features of DR is yet to appear. Among the few theories/models that try to describe the mechanism of DR, one is centered on the argument that DR arises from a competition between the surface charge and the curvature-dependent surface energy. Incorporating contributions from both of these effects, Lee et al. developed a modified Gibbs−Thompson equation that rationalizes the conversion of the polydisperse system into a monodisperse one.[10] However, this model ignores many factors such as the influence of surface-active ligands on the final size of the NPs. Another model that has appeared more recently tries to account for the role of organic ligands in a more comprehensive way by suggesting that the growth rates of nanocrystals having different sizes are affected to different extents because the solubility/diffusibility of monomers of the NP species is different in the layer of ligand molecules attached to the NPs compared with that of the bulk solution.[11] Such differences will have a great influence on the mobility of monomers to and from the NP surface, thereby influencing their size.

Here, the aspects that could have greater impact on the mobility of monomers are (1) the strength of interaction between the functional group of the ligand and the surface of the NP and (2) the strength of van der Waals (vdW) attractive forces existing between the organic ligands present on the surface of the NPs.[12,13] We hypothesized that we could gain useful insight into the influence of these two factors on the NP size by performing DR using multidentate ligands. In this context, Lee and co-workers have systematically studied the formation of self-assembled monolayers (SAMs) on Au(111) surfaces using three model ligands consisting of mono-, di-, and trithiol groups attached to one alkyl chain (Figure 1; **L1**, **L2**,

Received: November 4, 2016
Revised: January 25, 2017
Published: January 27, 2017

DOI: 10.1021/acs.langmuir.6b03998
Langmuir 2017, 33, 1943−1950

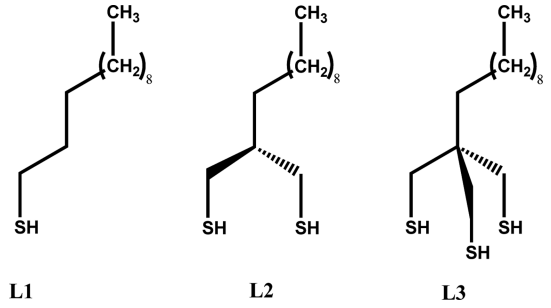

Figure 1. Structure of ligands used in this study for Au NP synthesis using DR.

and **L3**, respectively).[14−16] Their research led to the conclusion that among these three ligands, the tridentate ligands exhibited the lowest packing densities of alkyl chains as compared to the SAMs of bidentate and monodentate analogues.[14] However, the tridentate ligands showed the highest chain tilt from the surface normal so that the alkyl chains maintained vdW contact. In fact, the thermal stability of the tridentate ligand SAMs was found to be significantly higher than the thermal stability of those formed from bidentate and monodentate ligands, with the bidentate SAMs in turn being more thermally stable than the monodentate SAMs.[15] An analogous trend in thermal stability (i.e., tridentate > bidentate > monodentate) was also observed on colloidal gold particles.[16]

Given this context, the purpose of this study was to understand and compare the DR ability of *n*-alkanethiols (**L1**) with those of chelating bidentate and tridentate thiols (**L2** and **L3**, respectively), with the goal of providing a new insight into the influence of the temperature-dependent strength of the ligand surface binding on the NP size. It is important to note here that although the relationship between the size narrowing of NPs and the nature of the functional group of the organic ligand has been investigated via systematic studies,[17−19] information regarding the influence of binding strength variation on the NP size by using multidentate ligands in the DR process does not exist to the best of our knowledge.

EXPERIMENTAL PROCEDURE

Synthesis of Ligands. **L1** was purchased from Sigma-Aldrich and used as received; **L2** and **L3** were synthesized following reported procedures.[14,16]

Preparation of Au NPs. Au NPs were prepared using a well-known DR method.[8] A 0.025 g aliquot of didodecyldimethylammonium bromide (DDAB) was dissolved in 2.5 mL of 4-*tert*-butyltoluene (*t*bt). The gold salt $AuCl_3$ was dissolved in this solution through sonication to make a 0.01 M solution. This dark orange solution was reduced by dropwise addition of aqueous $NaBH_4$ (25 μL, 9.4 M) under vigorous stirring, which was continued for 1 h to ensure complete reduction. The NPs formed at this point will be referred to as the "as-prepared" system in the remainder of the text. Ligands were added to this as-prepared system maintaining the metal-to-ligand molar ratio at 1:20 and stirring the solution for 15 min at room temperature. Subsequently, these ligand-coated NPs were separated from the excess ligand, DDAB, and other reaction side products by precipitating with the addition of excess ethanol (7.5 mL). The precipitate was then dried and again redispersed in 2.5 mL of *t*bt. Another dose of respective ligands was added, maintaining a 1:20 metal-to-ligand molar ratio. The colloidal dispersions in *t*bt were then heated at selected temperatures (i.e., 60, 120, and 180 °C) for 1 h. The resultant NPs were characterized using transmission electron microscopy (TEM) and UV−visible (UV−vis) spectroscopy. For TEM, NP dispersions were drop-cast on a TEM grid after heating at different temperatures, and approximately 300 particles were analyzed for the calculation of the particle size distribution (PSD).

RESULTS

Gold NPs were synthesized using a well-known DR procedure.[4,8] The first step of this procedure involved preparation of a colloidal gold dispersion, termed "as-prepared" particles, in nonpolar organic solvents in the presence of the surfactant DDAB. These were separated into three portions, and to each portion of these particles, an aliquot of ligand **L1**, **L2**, or **L3** was added, maintaining a ligand/gold molar ratio of 20:1. These ligand-coated particles were then separated from the reagents and any reaction side products by precipitation. They were then subjected to the DR process by adding another portion of the respective ligand (again at a 20:1 ratio) followed by heating in an organic solvent (*t*bt) at a selected temperature. Interesting trends in particle sizes were observed after the addition of ligands and after heating the particles with the ligands, depending on the type of ligand used and the temperature at which the DR process was conducted. The details are presented below.

The TEM Analysis of the initial as-prepared Au NPs revealed that the particles were highly polydispersed (Figure 2). The presence of irregularly shaped particles was also evident. The first interesting observation in our experiments was the significant narrowing of the size distribution of the particles (Figure 3) when the ligands were merely added to the as-prepared particles. Subsequently, when **L1** was used as the ligand, upon heating the system at 60 °C, a significant decrease in the polydispersity of the NPs was observed, and smaller

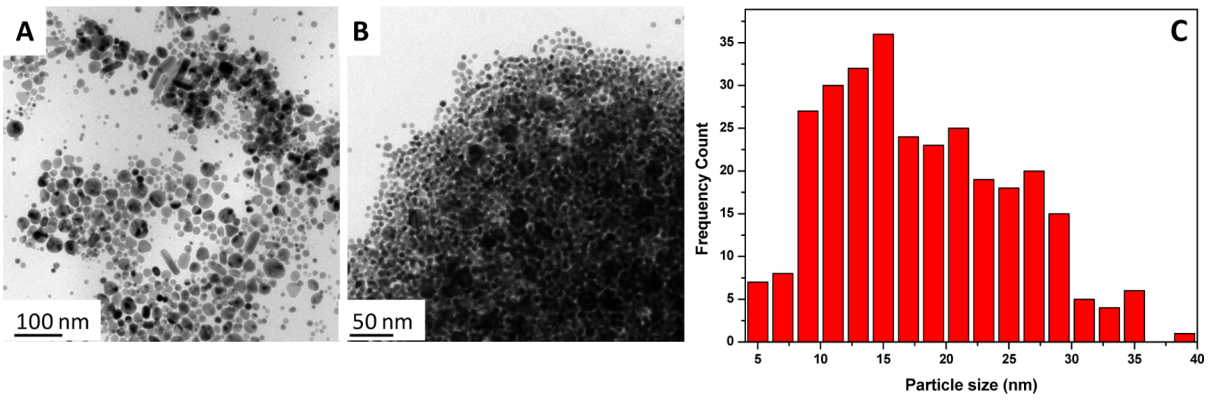

Figure 2. (A,B) TEM images and (C) particle size histograms of the as-prepared NP systems (i.e., before the addition of any thiol capping ligand).

DOI: 10.1021/acs.langmuir.6b03998
Langmuir 2017, 33, 1943−1950

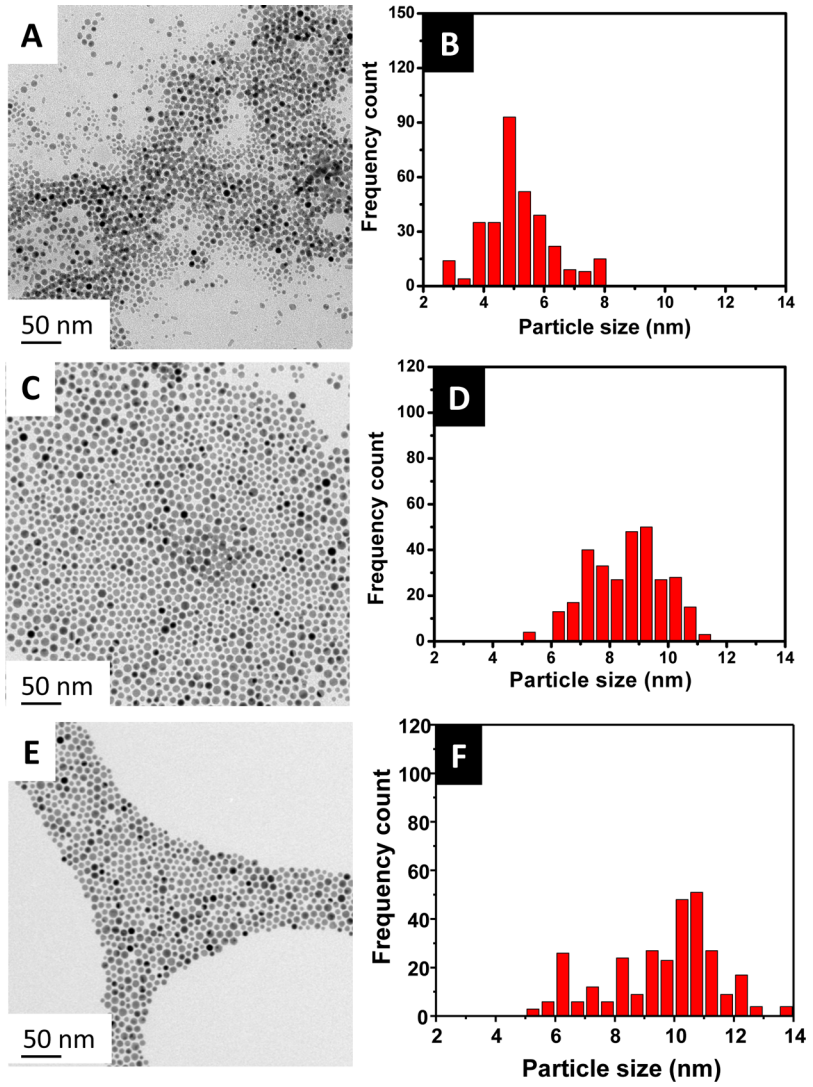

Figure 3. TEM images and particle size histograms of the Au NP systems obtained by adding ligands **L1** (A,B), **L2** (C,D), and by **L3** (E,F) at room temperature.

particle sizes of 4.8 ± 0.4 nm were obtained (Figure 4A–C), when compared with those obtained by the simple addition of **L1** at room temperature. With increasing coordination sites on the ligand, heating at 60 °C caused a decrease in the polydispersity of the system, but comparatively larger particles were obtained. For example, particle sizes of 9.3 ± 0.6 nm were obtained with **L2** (Figure 4D–F), and particle sizes of 10.3 ± 0.9 nm were obtained when **L3** was used (Figure 4G–I). Additional representative TEM images of the Au NPs obtained from the DR experiments with ligands **L1**, **L2**, and **L3** at 60 °C are provided in Figure S1. Compared with the data at 60 °C, an increase in the temperature to 120 °C caused a slight increase in the particle size (5.6 ± 0.5 nm) when **L1** was used as the ligand (Figures 5A–C and S2A–C); however, with **L2** and **L3**, significant decreases in the particle size were observed, which is quite interesting. For example, with **L2**, upon increasing the temperature from 60 to 120 °C, the particle sizes decreased from 9.3 ± 0.6 to 5.3 ± 0.7 nm (Figures 5D–F and S2D–F). Concurrently, a population of smaller particles (~3–5 nm) was observed to develop (highlighted portion of the image in Figure 5E). Similarly, with **L3**, the sizes of the particles decreased from 10.3 ± 0.9 to 5.3 ± 0.8 nm (Figures 5G–I and S2G–I). Here again, similar to the results from **L2**, small particles (~3–5 nm) were also observed to appear (highlighted portion of the image in Figure 5H). A further increase in the temperature to 180 °C caused a small increase in the particle size and polydispersity (7.4 nm ± 0.7) when **L1** was used as the ligand (Figures 6A–C and S3A–C). However, with **L2** and **L3**, there were no significant differences in the sizes of both the large and small particles compared with those obtained at 120 °C, but the number of the smaller particles and the overall polydispersity increased significantly (Figures 6D–I and S3D–I).

We also recorded the UV–vis spectra after performing DR with the different ligands at different temperatures. In the case of the as-prepared particles, a peak at 530 nm corresponding to the localized surface plasmon resonance was observed.[20] However, heating the as-prepared particles with **L1**, **L2**, and **L3** led to a small blue shift in the peak position at all temperatures. Furthermore, we did not observe any clear trend with respect to the position of the peak or its full width at half-maximum (Figure S4).

DOI: 10.1021/acs.langmuir.6b03998
Langmuir 2017, 33, 1943–1950

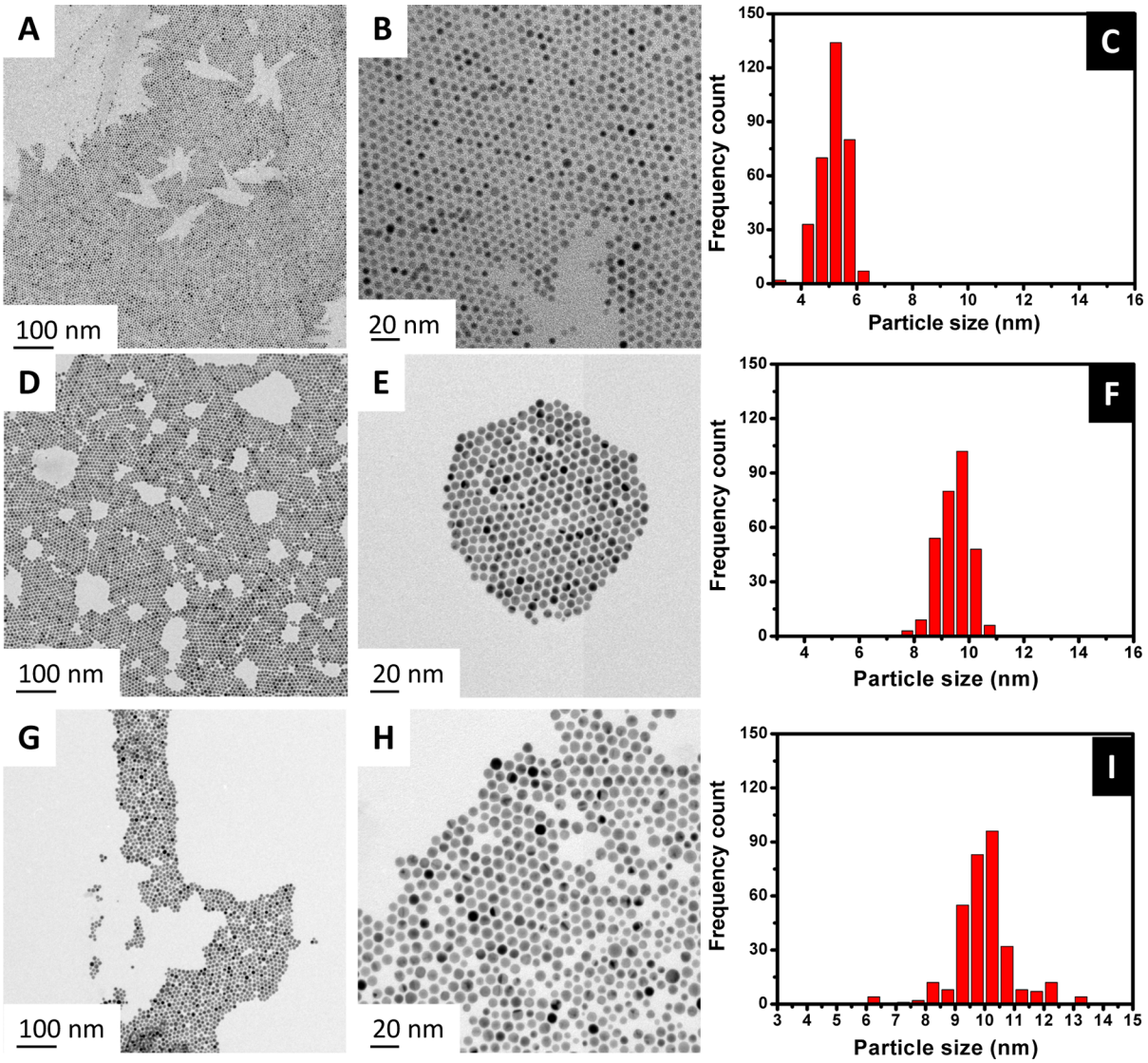

Figure 4. TEM images and the respective particle size histograms of NPs obtained at 60 °C using ligands **L1** (A–C), **L2** (D–F), and **L3** (G–I).

DISCUSSION

The as-prepared particles are polydisperse in nature, with their sizes varying from 5 to 40 nm (Figure 2C). For all ligand systems, the mere addition of ligands **L1**, **L2**, or **L3** to DDAB-capped NPs at room temperature leads to a decrease in the polydispersity (Figure 3). The narrowing size distribution of the gold particles is due to the well-known etching process that thiols are known to cause.[21] However, the size distributions (5.2 ± 1.1 nm for **L1**, 8.4 ± 1.3 nm for **L2**, and 9.5 ± 1.9 nm for **L3**) obtained at this stage are not as narrow as expected from the DR process.[5] Thus, room temperature etching itself cannot plausibly explain the formation of monodisperse particles. In an earlier study, we established that temperatures of 60–120 °C offered conditions suitable for the DR process to operate, which leads to a significant narrowing in the PSD.[22] Consistent with the previous studies, we found that heating the as-prepared polydisperse NPs at 60 °C in the presence of all three ligand types led to a decrease in the NP size and a significant narrowing of the size distribution. We wish to note here that the changes observed in the peak position of the UV–vis spectra (from ∼530 to ∼520 nm) also indicate the narrowing of the size distribution when the DR process was carried out at all of the temperatures (Figure S4). Unfortunately, it is difficult to deduce small changes in particle sizes using the UV–vis spectral analysis. Therefore, we relied on the particle size analysis using the TEM images. From these analyses, it can be concluded that carrying out the DR process at 60 °C induces a significant narrowing of the size distribution, although the sizes of the NPs obtained in each case vary and display some interesting trends, wherein smaller particles are obtained with **L1** when compared with those obtained with **L2** or **L3**.

Although a complete understanding of the DR process still eludes us, the available evidence suggests that it involves the modification of both smaller and larger particles to a certain extent. Among them, the larger particles, featured with defects such as twinning boundaries and stacking faults, facilitate the ligands to access the interior sites of the particles, first leading to their breaking into smaller particles. Second, an oxidation reaction between the thiol molecules and the NPs occurs at the surface of the particle, forming thiolates of gold/gold clusters that dissolve in the solvent. Similarly, the smallest (more reactive) particles get completely dissolved, concomitantly forming thiolates because of their higher surface energies.

DOI: 10.1021/acs.langmuir.6b03998
Langmuir 2017, 33, 1943–1950

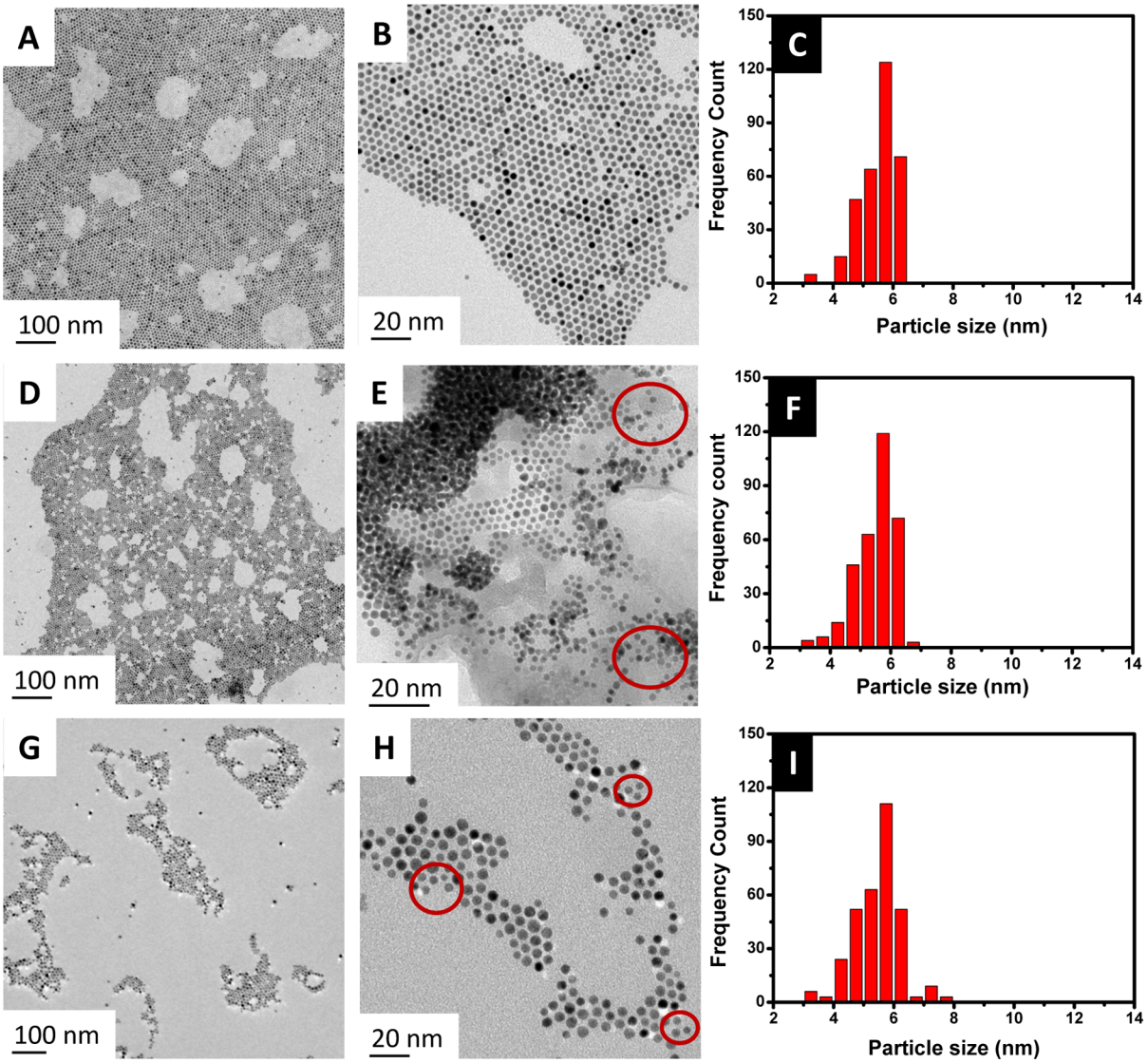

Figure 5. TEM images and the respective particle size histograms of NPs obtained at 120 °C using ligands **L1** (A–C), **L2** (D–F), and **L3** (G–I). The circled portions in (E) and (H) show the presence of smaller particles.

These dissolved thiolates get deposited on other relatively more stable smaller particles, which leads to their growth.[17]

Of the ligands examined in the present study, **L1** has been known to display the least thermal stability on both planar and three-dimensional gold surfaces.[23] Therefore, it can desorb from the surface easily and plausibly etch readily, suggesting that it might be the most effective DR agent. On the contrary, **L2** and **L3** bind strongly to the NP surfaces, which might limit their ability to etch.[24] Thus, we conclude that when the DR process is carried out at 60 °C with **L2** and **L3** ligands, larger particles are preferentially formed because of the poor etching and the hampered diffusibility of the small number of Au clusters/atoms that have been etched out through the strongly bound bidentate and tridentate ligands on the surface of the NPs.[24,25]

Interesting trends in the particle size variations were observed on heating the NPs at higher temperatures. More specifically, increasing the temperature to 120 °C with **L1** did not alter the particle size or the size distribution in any significant way. On the other hand, at 120 °C, with **L2** and **L3**, the formation of many small particles was observed along with the decrease in the mean particle size. It has been suggested that in the case of DR, for a given metal–ligand system, one preferred size exists when the reaction is carried out at relatively mild temperatures. In the case of gold–monodentate thiols (especially dodecanethiol), the preferred size is ∼5 nm in the temperature range of 60–120 °C.[17] Our results also clearly support this conclusion, and 60 °C and 120 °C, the particle sizes obtained with **L1** were around 5 nm. Interestingly, the particle sizes obtained with **L2** and **L3** were also around 5 nm when the DR was carried out at 120 °C. We surmise that at this temperature, the bidentate and tridentate ligands also begin to desorb from the surface of the NPs, and while doing so, they act as gold surface etchants and carry with them atoms/clusters of Au from the large particles (digestion) into solution.[26] We propose that with **L2** and **L3** molecules, the ∼5 nm size observed with the majority of particles is mainly due to the enhanced etching of the larger particles. This contention is supported by the presence of smaller particles observed with these two ligands at 120 °C. Our earlier study revealed that with monodentate thiol, the time taken for the realization of best results with DR in the temperature range of 60–120 °C is

DOI: 10.1021/acs.langmuir.6b03998
Langmuir 2017, 33, 1943–1950

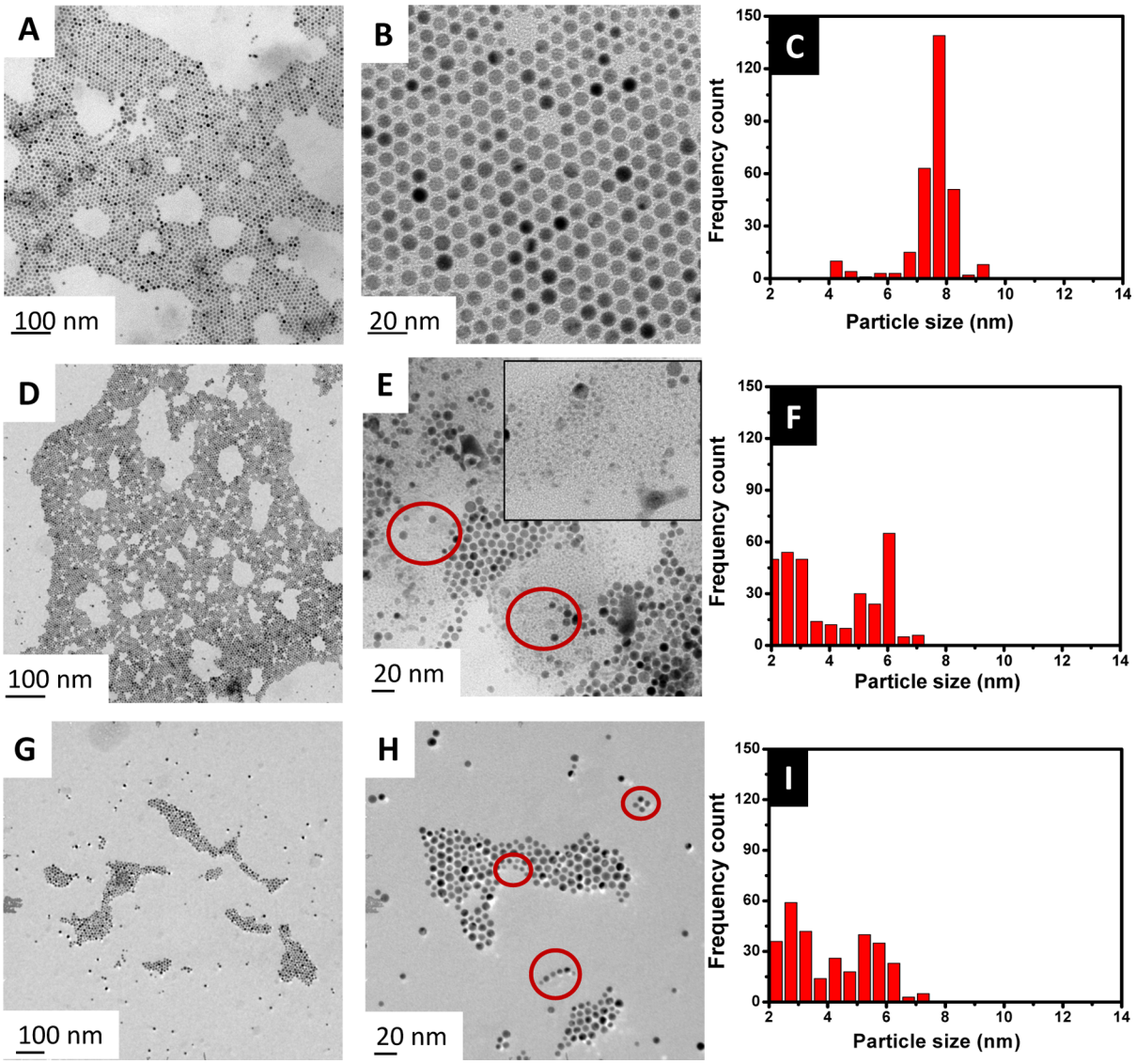

Figure 6. TEM images and the respective particle size histograms of NPs obtained at 180 °C using ligands **L1** (A–C), **L2** (D–F), and **L3** (G–I). The circled portions in E and H and the inset in (E) show the presence of smaller particles.

~1 h. Increasing the time of heating at lower temperatures does not cause much change in the size or the size distribution.[22]

As we increased the temperature to 180 °C, an increase in the particle size and size distribution was observed with **L1**. As mentioned previously, **L1** has the least thermal stability on gold surfaces, and thus when particles capped by **L1** are heated at 180 °C, more thiol molecules are able to desorb from the gold surface,[21] which leads to the formation of particles that are devoid of capping ligands that undergo coalescence and particle aggregation. This rationalizes the increase in the particle size when the DR process is carried out with **L1** at elevated temperatures and is consistent with our previous observations.[22] With **L2** and **L3**, the increase in temperature to 180 °C led to a decrease in the mean particle size. This decrease in the particle size and the formation of smaller particles at 180 °C can be largely attributed to the dominant etching process effected by these ligands. In a traditional DR process carried with monodentate alkanethiols at lower temperatures, these clusters/atoms are deposited on a smaller particle leading to an increase in size (ripening). In the present case with the **L2** and **L3** molecules, the etching process does seem to occur at elevated temperatures, leading to the observed decrease in the mean particle size of the larger particles. Our previous results indicate that at a higher temperature, the monodispersed state is reached much faster with the monodentate ligands, but continuing the heating at a higher temperature for longer periods of time leads to aggregation and increased polydispersity, indicating a cross-over from the traditional DR process to Ostwald ripening process.

Interestingly, in the present instance with **L2** and **L3** ligands, the smaller particles do not seem to grow in size, but their number density seems to increase as the temperature is increased from 120 to 180 °C. This observation suggests that whereas the etching (digestion) process is still proceeding, the ripening process is compromised with the **L2** and **L3** ligands, even at elevated temperatures, which gives rise to the remnant small particles. This phenomenon could be ascribed to the fact that as soon as a naked gold surface site is formed via the desorption of a bidentate/tridentate ligand, the same site is passivated by other thiol groups present on the surface. In fact, it has been found with these multidentate ligands that a significant portion of the anchoring groups is still not bound to

DOI: 10.1021/acs.langmuir.6b03998
Langmuir 2017, 33, 1943–1950

the gold surface.[27,28] These free chelating arms might passivate the naked gold surfaces being formed, thus preventing the deposition of small atoms/clusters on the existing NP surface, hampering their growth. This increase in the number of small particles is reflected as an increase in the polydispersity around 1 h. We did not continue heating for a longer time duration because reaching the polydispersed state indicates the onset of Ostwald ripening process, as noted in our previous study.[22]

The loss in the stabilization energy, if any, due to the desorption of these ligands and the resulting sparse packing density of the alkyl chains could be compensated by a higher chain tilt from the surface normal, as has been previously reported.[14] The remnants of the gold atoms/clusters present in solution, which are not deposited on the existing gold NPs, rationalize the presence of small particles and their increased number density at higher temperatures. Formation of such small particles/clusters can be of interest in the background of extensive literature that is emanating from studies related to thiolate-protected ultrasmall gold nanoclusters[29−31] and warrants further study.

CONCLUSIONS

We have unambiguously demonstrated that compared with multidentate thiol ligands, monodentate thiols are better DR agents. This study revealed that the final particle size after DR is influenced by the chelating strength and thermal stability of the thiol groups of the multidentate ligands on the NP surface and the associated ability/disability of the thiol-etched gold atoms/clusters to be deposited on the existing particle surfaces.

ASSOCIATED CONTENT

Supporting Information

The Supporting Information is available free of charge on the ACS Publications website at DOI: 10.1021/acs.langmuir.6b03998.

TEM images of Au NP systems obtained at 60, 120, and 180°C with ligands **L1**, **L2**, and **L3** and UV−vis spectra of the as-prepared Au NPs compared with those obtained after DR with ligands **L1**, **L2**, and **L3** at different temperatures (PDF)

AUTHOR INFORMATION

Corresponding Author

*E-mail: pl.bhagavatula@ncl.res.in. Phone: +91-20-25902013. Fax: +91-20-25902636.

ORCID

T. Randall Lee: 0000-0001-9584-8861

Bhagavatula L. V. Prasad: 0000-0002-3115-0736

Notes

The authors declare no competing financial interest.

ACKNOWLEDGMENTS

The research at the University of Houston was generously supported by the National Science Foundation (CHE-1411265), the Robert A. Welch Foundation (Grant No. E-1320), and the Texas Center for Superconductivity. We thank CSIR, New Delhi for financial support through the 12th five-year plan project CSC-0134. The authors acknowledge the Indo-US symposium on "Molecular Materials" held in Bangalore during July 2013 that inspired this collaborative work.

REFERENCES

(1) Brust, M.; Walker, M.; Bethell, D.; Schiffrin, D. J.; Whyman, R. Synthesis of thiol-derivatised gold nanoparticles in a two-phase liquid−liquid system. *J. Chem. Soc., Chem. Commun.* **1994**, 801−802.

(2) Goulet, P. J. G.; Lennox, R. B. New insights into Brust−Schiffrin metal nanoparticle synthesis. *J. Am. Chem. Soc.* **2010**, *132*, 9582−9584.

(3) Li, Y.; Zaluzhna, O.; Tong, Y. J. Identification of a source of size polydispersity and its solution in Brust−Schiffrin metal nanoparticle synthesis. *Chem. Commun.* **2011**, *47*, 6033−6035.

(4) Lin, X. M.; Sorensen, C. M.; Klabunde, K. J. Digestive ripening, nanophase segregation and superlattice formation in gold nanocrystal colloids. *J. Nanopart. Res.* **2000**, *2*, 157−164.

(5) Prasad, B. L. V.; Stoeva, S. I.; Sorensen, C. M.; Klabunde, K. J. Digestive Ripening, Nanophase Segregation and Superlattice Formation in Gold Nanocrystal Colloids. *Langmuir* **2002**, *18*, 7515−7520.

(6) Jin, R.; Qian, H.; Wu, Z.; Zhu, Y.; Zhu, M.; Mohanty, A.; Garg, N. Size focusing: A methodology for synthesizing atomically precise gold nanoclusters. *J. Phys. Chem. Lett.* **2010**, *1*, 2903−2910.

(7) Kalikmanov, V. I. Classical Nucleation Theory. In *Nucleation Theory*; Springer, 2013; pp 17−41.

(8) Sidhaye, D. S.; Prasad, B. L. V. Many manifestations of digestive ripening: Monodispersity, superlattices and nanomachining. *New J. Chem.* **2011**, *35*, 755−763.

(9) Bhaskar, S. P.; Vijayan, M.; Jagirdar, B. R. Size Modulation of Colloidal Au Nanoparticles via Digestive Ripening in Conjunction with a Solvated Metal Atom Dispersion Method: An Insight into Mechanism. *J. Phys. Chem. C* **2014**, *118*, 18214−18225.

(10) Lee, D.; Park, S.; Lee, J.; Hwang, N. A theoretical model for digestive ripening. *Acta Mater.* **2007**, *55*, 5281−5288.

(11) Clark, M. D. Growth laws for surfactant-coated nanocrystals: Ostwald ripening and size focusing. *J. Nanopart. Res.* **2014**, *16*, 1−8.

(12) Salem, L. Attractive forces between long saturated chains at short distances. *J. Chem. Phys.* **1962**, *37*, 2100−2113.

(13) Badia, A.; Cuccia, L.; Demers, L.; Morin, F.; Lennox, R. B. Structure and Dynamics in Alkanethiolate Monolayers Self-Assembled on Gold Nanoparticles: A DSC, FT-IR, and Deuterium NMR Study. *J. Am. Chem. Soc.* **1997**, *119*, 2682−2692.

(14) Park, J.-S.; Vo, A. N.; Barriet, D.; Shon, Y.-S.; Lee, T. R. Systematic Control of the Packing Density of Self-Assembled Monolayers Using Bidentate and Tridentate Chelating Alkanethiols. *Langmuir* **2005**, *21*, 2902−2911.

(15) Breslow, R.; Belvedere, S.; Gershell, L.; Leung, D. The chelate effect in binding, catalysis, and chemotherapy. *Pure Appl. Chem.* **2000**, *72*, 333−342.

(16) Srisombat, L.-o.; Zhang, S.; Lee, T. R. Thermal Stability of Mono-, Bis-, and Tris-Chelating Alkanethiol Films Assembled on Gold Nanoparticles and Evaporated "Flat" Gold. *Langmuir* **2010**, *26*, 41−46.

(17) Jose, D.; Matthiesen, J. E.; Parsons, C.; Sorensen, C. M.; Klabunde, K. J. Size focusing of nanoparticles by thermodynamic control through ligand interactions. Molecular clusters compared with nanoparticles of metals. *J. Phys. Chem. C* **2012**, *3*, 885−890.

(18) Sahu, P.; Prasad, B. L. V. Effect of digestive ripening agent on nanoparticle size in the digestive ripening process. *Chem. Phys. Lett.* **2012**, *525−526*, 101−104.

(19) Stoeva, S. I.; Zaikovski, V.; Prasad, B. L. V.; Stoimenov, P. K.; Sorensen, C. M.; Klabunde, K. J. Reversible Transformations of Gold Nanoparticle Morphology. *Langmuir* **2005**, *21*, 10280−10283.

(20) Mulvaney, P. Surface Plasmon Spectroscopy of Nanosized Metal Particles. *Langmuir* **1996**, *12*, 788−800.

(21) Biener, M. M.; Biener, J.; Friend, C. M. Revisiting the S−Au(111) Interaction: Static or Dynamic? *Langmuir* **2005**, *21*, 1668−1671.

(22) Sahu, P.; Prasad, B. L. V. Time and Temperature Effects on the Digestive Ripening of Gold Nanoparticles: Is There a Crossover from Digestive Ripening to Ostwald Ripening? *Langmuir* **2014**, *30*, 10143−10150.

(23) Valášek, M.; Lindner, M.; Mayor, M. Rigid multipodal platforms for metal surfaces. *Beilstein J. Nanotechnol.* **2016**, *7*, 374−405.

DOI: 10.1021/acs.langmuir.6b03998
Langmuir 2017, 33, 1943−1950

(24) Fertitta, E.; Voloshina, E.; Paulus, B. Adsorption of multivalent alkylthiols on Au(111) surface: Insights from DFT. *J. Comput. Chem.* **2014**, *35*, 204−213.
(25) Oh, E.; Susumu, K.; Mäkinen, A. J.; Deschamps, J. R.; Huston, A. L.; Medintz, I. L. Colloidal Stability of Gold Nanoparticles Coated with Multithiol-Poly(ethylene glycol) Ligands: Importance of Structural Constraints of the Sulfur Anchoring Groups. *J. Phys. Chem. C* **2013**, *117*, 18947−18956.
(26) Hostetler, M. J.; Templeton, A. C.; Murray, R. W. Dynamics of Place-Exchange Reactions on Monolayer-Protected Gold Cluster Molecules. *Langmuir* **1999**, *15*, 3782−3789.
(27) Wei, L.; Tiznado, H.; Liu, G.; Padmaja, K.; Lindsey, J. S.; Zaera, F.; Bocian, D. F. Adsorption Characteristics of Tripodal Thiol-Functionalized Porphyrins on Gold. *J. Phys. Chem. B* **2005**, *109*, 23963−23971.
(28) Kittredge, K. W.; Minton, M. A.; Fox, M. A.; Whitesell, J. K. α-Helical polypeptide films grown from sulfide or thiol linkers on gold surfaces. *Helv. Chim. Acta* **2002**, *85*, 788−798.
(29) Goswami, N.; Yao, Q.; Chen, T.; Xie, J. Mechanistic exploration and controlled synthesis of precise thiolate−gold nanoclusters. *Coord. Chem. Rev.* **2016**, *329*, 1−15.
(30) Chen, T.; Luo, Z.; Yao, Q.; Yeo, A. X. H.; Xie, J. Synthesis of thiolate-protected Au nanoparticles revisited: U-Shape trend between the size of nanoparticles and thiol-to-Au ratio. *Chem. Commun.* **2016**, *52*, 9522−9525.
(31) Luo, Z.; Nachammai, V.; Zhang, B.; Yan, N.; Leong, D. T.; Jiang, D.-e.; Xie, J. Toward Understanding the Growth Mechanism: Tracing All Stable Intermediate Species from Reduction of Au(I)−Thiolate Complexes to Evolution of Au_{25} Nanoclusters. *J. Am. Chem. Soc.* **2014**, *136*, 10577−10580.

DOI: 10.1021/acs.langmuir.6b03998
Langmuir 2017, 33, 1943−1950